Phase Segregation in Gradient Copolymer Melts

Michelle D. Lefebvre, Monica Olvera de la Cruz, and Kenneth R. Shull*

Department of Materials Science and Engineering, Northwestern University, Evanston, Illinois 60208

Received August 6, 2003; Revised Manuscript Received November 14, 2003

ABSTRACT: Local segregation in melts of copolymers with composition gradients along their backbones is analyzed. The transition to a lamellar periodic structure as the effective degree of incompatibility χN increases is studied for symmetric copolymers with various composition gradients. A numerical self-consistent mean-field (SCMF) technique is used to characterize the ordered lamellar state in the weak and strong segregation regimes, and the random phase approximation (RPA) is used to calculate the scattering function analytically and find the location of the critical order−disorder transition for each melt. The critical point increases from $(\chi N)_c = 10.495$ for block copolymers to $(\chi N)_c = 29.25$ for a fully tapered linear gradient copolymer. For broad composition gradients the equilibrium lamellar repeat length is shorter for a given value of χN, and the unit cell composition profile is more sinusoidal. The dependence of the equilibrium repeat distance on χN is nearly universal when renormalized by the critical point of each copolymer.

Introduction

The synthesis of copolymers of various molecular weights and compositions has led to the ability to create new materials with unique bulk and surface properties.[1,2] For block copolymers, the chemical connectivity of the two immiscible blocks drives the formation of locally segregated domains. In the melt state, these segregated domains form periodic structures with long-range symmetry. One-dimensional lamellar, two-dimensional hexagonally closed packed cylinders, and three-dimensional structures are both predicted and observed experimentally.[3] These periodic structures are also observed in a large variety of copolymer architectures such as triblock, graft, star, and certain random copolymers.[4−9]

The physical properties of A−B copolymer melts are determined by the average number of monomers per chain, N, the degree of incompatibility between the A and B repeat units per thermal energy, χ, the average fraction of A repeat units in the chains, f, and the asymmetry of the constituent repeat units.[10] The behavior of symmetric A−B block copolymer melts is well understood. When χN is lower than a critical value denoted by $(\chi N)_c$, the melt is isotropic. Here, the chains are ideal with dimensions given by the unperturbed radius of gyration, denoted by $R_g = aN^{1/2}$, where a is the characteristic monomer size. For simplicity, a is considered equal for the A and B monomers. For symmetric diblock copolymer melts, the mean-field prediction is $(\chi N)_c = 10.495$.[11] When χN is increased above this value, a long-range lamellar structure of periodicity L is formed. At very large values of χN the lamellae have narrow interfaces and a periodicity that scales as $L \sim \chi^{1/6}N^{2/3}$.[12] In this strongly segregated regime the chains are significantly perturbed from their ideal Gaussian conformations.

New types of copolymers termed gradient copolymers have been synthesized by living free radical polymerization methods, including atom transfer radical polymerization[13−15] and nitroxide-mediated free radical polymerization.[16−18] Gradient copolymers have a controlled composition gradient along the backbone of the chain. The two ends may consist of pure A and B monomers for example, with a gradual variation between these two extremes. If the length of this composition gradient is large, one may expect different density profiles inside the unit cell of the periodic structure than those found in traditional block copolymers. In this paper we analyze the phase separation in symmetric gradient copolymer melts with different gradient profiles in both the ordered and disordered states. We will first define the gradient copolymers and the theoretical description of the formation of one-dimensional lamellae. We then determine the scattering function of a monodisperse melt of gradient copolymers in the disordered state and the location of the transition to the ordered state by using the random phase approximation (RPA). We also determine the equilibrium size L and density profile of the periodic structure as functions of both the fractional length of the gradient and χN by using a self-consistent mean-field (SCMF) technique. The results from these calculations are used to examine the scaling behavior of L as a function of χN, where appropriate normalization gives a near-universal curve.

Theoretical Formulation

Gradient copolymers are defined by the composition profile for repeat unit A along the chain backbone. Here, the function $g(n)$ describes the composition at repeat unit n in a chain of N repeat units. The overall volume fraction f of A repeat units is the average value of g:

$$f = \frac{1}{N}\int_0^N g(n)\,\mathrm{d}n \tag{1}$$

For gradient copolymers an additional parameter λ is introduced to describe the fractional length of the gradient along the chain. For example, $\lambda = 0$ means there is no gradient and denotes a block copolymer. Conversely, $\lambda = 1$ means the gradient extends along the entire chain. The way in which the composition varies can be represented in many ways. In this paper, we consider two types of gradient: linear and hyperbolic tangent (tanh). For linear gradient copolymers, this discussion is limited to $f = 0.5$ and $\lambda = 0$, 0.5, and 1.

* Corresponding author: e-mail k-shull@northwestern.edu.

10.1021/ma035141a CCC: $27.50
Published on Web 01/16/2004

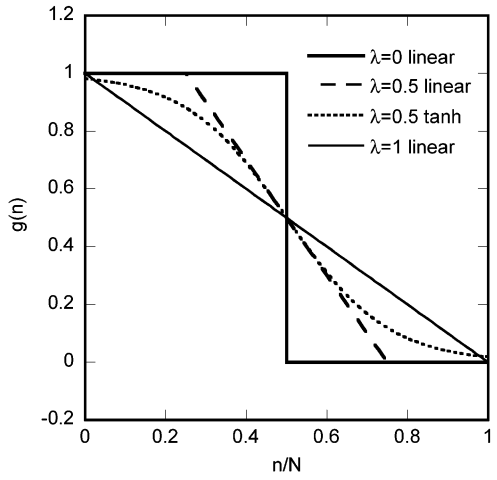

Figure 1. Composition profile $g(n)$ along the normalized length of the chain n/N for four gradient copolymers. Linear gradients are shown for $\lambda = 0$, $\lambda = 0.5$, and $\lambda = 1$, and a tanh gradient is shown for $\lambda = 0.5$.

For these cases, the profile g can be written as

$$g(n) = \begin{cases} 1 & \frac{n}{N} < 0.5(1-\lambda) \\ 0.5 + \frac{1}{\lambda}\left(0.5 - \frac{n}{N}\right) & 0.5(1-\lambda) < \frac{n}{N} < 0.5(1+\lambda) \\ 0 & \frac{n}{N} > 0.5(1+\lambda) \end{cases} \quad (2)$$

For the tanh gradient profile the form of $g(n)$ is such that the slope at $n/N = 0.5$ is the same as a linear profile with the same λ. One tanh gradient copolymer profile is considered here, with $f = 0.5$ and $\lambda = 0.5$:

$$g(n) = 0.5 + 0.5 \tanh\left(\frac{1}{\lambda}\left(1 - \frac{2n}{N}\right)\right) \quad (3)$$

The values of $g(n)$ for the four copolymers are plotted in Figure 1.

In a melt of copolymers of the same length and the same composition and gradient, the overall density of monomers is constant. However, there will be local fluctuations in the dimensionless A and B segment densities ρ_A and ρ_B that lead to microphase separation into lamellar structures when χN increases above the critical value $(\chi N)_c$. When the product of χ and N is small, entropy dominates and the melt is disordered. At increasing chain length or decreasing temperature (increasing χN), a transition to an ordered phase occurs to decrease the number of unfavorable A and B monomer contacts. In the disordered region, the fluctuations leading to the formation of these ordered phases can be characterized by the density−density correlation function $S(r)$, which can be found using an RPA method. In the ordered region, the density fluctuations are characterized by their long-range equilibrium periodicity and density profile, which can be accessed using SCMF theory.

Disordered Region. The random density fluctuations in the disordered phase are described by the density−density correlation function $S(r)$. The Fourier transform of $S(r)$, the scattering function $S(k)$, can be obtained experimentally by scattering techniques. The scattering function can also be obtained analytically using an RPA method, which assumes that the chain conformations obey random walk statistics. The connectivity of the A and B monomers leads to a maximum in the monomer fluctuations at length scales on the order of R_g. In the mean-field model of Leibler,[11] the fluctuations grow as χN approaches the order−disorder transition at $(\chi N)_c$, and the scattering intensity $S(k)$ has a peak at a critical wavevector, k_c, near $1/R_g$. $S(k_c)$ grows rapidly as χN approaches $(\chi N)_c$, but k_c remains constant. The intensity of the scattering function at the critical wavevector diverges to infinity when the disordered fluctuations become an ordered structure at $(\chi N)_c$. This transition marks the spinodal line in the phase diagram. For $f = 0.5$, this is also the order−disorder transition, making it a critical point.

For finite size chains a self-consistent mean-field calculation of the concentration fluctuations (Hartree approach) gives a small correction to the scaling of k_c in the disordered state[19] that has been observed experimentally.[20] This slight χN-dependent correction to k_c suggests that the chains are slightly stretched before the microphase segregation transition.[19,21] In this paper we do not include this correction.

To find an analytical form of the scattering function in the disordered region at $f = 0.5$, $\chi N < (\chi N)_c$, we use the method developed originally by Leibler for block copolymers,[11] generalized here to treat gradient copolymers. The RPA scattering function is written in terms of the Fourier transform of the single-chain correlation functions between the i and j monomers, $\hat{g}_{ij}$. It is convenient to normalize these single-chain correlation functions by defining $g_{ij} = \hat{g}_{ij}/N$. For a homopolymer, g_{AA} is the Debye function:

$$g_{AA} = \frac{1}{N^2}\int_0^N \mathrm{d}n \int_0^N \mathrm{d}n'\, \mathrm{e}^{(-k^2a/6)|n-n'|} = \frac{2}{x^2}(x + \mathrm{e}^{-x} - 1) \quad (4)$$

with

$$x = k^2 R_g{}^2 = \frac{k^2 N a^2}{6} \quad (5)$$

where R_g is the radius of gyration of a chain with N monomers, k is the wavevector, and a is the statistical segment length of a monomer. For gradient copolymers, the correlation functions must be modified by the composition profile of the polymer, $g(n)$.

$$g_{AA} = \int_0^N \mathrm{d}n \int_0^N \mathrm{d}n'\, \mathrm{e}^{(-k^2a/6)|n-n'|} g(n)\, g(n') \quad (6)$$

$$g_{AB} = \int_0^N \mathrm{d}n \int_0^N \mathrm{d}n'\, \mathrm{e}^{(-k^2a/6)|n-n'|} g(n)(1 - g(n')) \quad (7)$$

Equations 6 and 7 are general and can be solved numerically for any gradient distribution. For linear gradient profiles, the correlation functions can be found analytically, shown here for $\lambda = 1$:

$$g_{AA} = \frac{2N^2}{x^4}\left(\frac{x^3}{3} - \frac{x^2}{2} - x\mathrm{e}^{-x} - \mathrm{e}^{-x} + 1\right) \quad (6a)$$

$$g_{AB} = \frac{2N^2}{x^4}\left(\frac{x^3}{6} + \frac{x^2}{2}\mathrm{e}^{-x} + x\mathrm{e}^{-x} + \mathrm{e}^{-x} - 1\right) \quad (7a)$$

For linear gradient copolymers with $\lambda < 1$, the correlation functions can be found analytically in the same manner used for $\lambda = 1$, while also accounting for the

effects of the pure A and pure B segments at the ends of the chains. This method is similar to the method used by Mayes and Olvera de la Cruz to find the correlation functions for triblock copolymers, where the behavior of the midblock is changed by the effects of the end blocks.[6]

For block and gradient copolymers, the inverse scattering function $S^{-1}(k)$ is a function of the single-chain correlation functions and is written as

$$S^{-1}(k) = \frac{1}{N}(F(x) - 2\chi N) \tag{8}$$

For symmetric copolymers, $g_{AA} = g_{BB}$ and $g_{AB} = g_{BA}$, so $F(x)$ can be written as

$$F(x) = \frac{2g_{AA} + 2g_{AB}}{g_{AA}^2 + g_{AB}^2} \tag{9}$$

After calculating g_{AA} and g_{AB} for the copolymers, eqs 8 and 9 can be used to find the inverse scattering function. The scattering function diverges at the order−disorder transition, so the inverse scattering function will be zero at the transition. Thus, the critical point is at $(\chi N)_c$ and k_c, where $S^{-1}(k_c) = 0$.

Ordered Region. We used the self-consistent mean-field approach formulated previously[12,22−24] and extended to gradient copolymers at interfaces by Shull.[25] We modified the approach described by Shull to treat gradient copolymers in melts. Only symmetric gradient copolymers with $f = 0.5$ are studied, so only lamellar symmetries are considered, where the composition modulation is in a single direction. The system is divided along this direction into layers of width a, where a is the statistical segment length of the polymer. The layers are labeled with the index $i = 1, 2, ..., L'$, and the segments along the polymer chain are labeled with the index $j = 1, 2, ..., N$.

The location of the polymer chain is governed by the probability distribution functions $q_1(i,j)$ and $q_2(i,j)$ that describe the probability of finding a segment j in the layer i. The segments are counted from the end of the chain, and there is a separate distribution function starting from each end. Segments starting from the A end of the chain are described by q_1, and segments starting from the B end of the chain are described by q_2. The connectivity of the chain results in a recursive relationship for the distribution functions. If a segment j is in layer i, then the segment $j - 1$ must be in layer $i - 1$, i, or $i + 1$, so for a three-dimensional lattice, the following recursion relation can be written for q_1 and q_2:

$$q(i,j) = \left(\frac{1}{6}q(i-1, j-1) + \frac{1}{6}q(i+1, j-1) + \frac{4}{6}q(i, j-1)\right)\exp(-w(i,j)/k_BT) \tag{10}$$

Equation 10 is the discretized form of the modified diffusion equations developed by Edwards[22] and utilized by Helfand,[12,23] Hong and Noolandi,[24] and others:

$$\frac{dq(z,n)}{dn} = \frac{a^2}{6}\frac{d^2q(z,n)}{dz^2} - w(z,n)\,q(z,n) \tag{11}$$

In the diffusion equation, z and n are the continuous forms of the variables i and j. In both equations, w is the mean field created by the surrounding monomers at segment j and layer i. The effect of the field depends on both the local composition of the chain, $g(j)$, and the surrounding composition in that layer, $\phi(i)$:

$$w(i,j) = \chi(g(j) - \phi_A(i))^2 - \Delta w(i) \tag{12}$$

It is also modified by $\Delta w(i)$, a constraint to enforce the incompressibility of the melt in each layer:

$$\Delta w(i) = \zeta(1 - \phi_A(i) - \phi_B(i)) \tag{13}$$

The parameter ζ is related to the compressibility of the melt. The volume fractions of A and B repeat units are obtained by summing the contribution from all possible chain segments or all possible junction points of the two distribution functions q_1 and q_2. To account for the composition variation along the chain, the volume fractions are modified by g:

$$\phi_A(i) = \frac{1}{N}\sum_{j=1}^{N} g(j)\, q_1(i,j)\, q_2(i, N-j) \tag{14}$$

$$\phi_B(i) = \frac{1}{N}\sum_{j=1}^{N} (1 - g(j)) q_1(i,j)\, q_2(i, N-j) \tag{15}$$

These equations must all be obeyed simultaneously, and they must be solved numerically for ϕ_A and ϕ_B. The free energy per chain f is obtained from Δw and is analogous to an interfacial free energy:

$$f = \frac{N}{L'}\sum_{i=1}^{L'} \Delta w(i) \tag{16}$$

For a given value of χN, the equilibrium lamellar repeat period L is obtained as the value of L' that minimizes the free energy. The behavior of L can then be examined as χN is increasing above $(\chi N)_c$. This SCMF formulation is advantageous because it is easily extended to multicomponent systems. The quadratic form of eq 12 is equivalent to the linear form that is often used, as shown previously.[25]

Results and Discussion

Disordered Region. RPA was used to calculate the inverse scattering function analytically for the block copolymer and two linear gradient copolymers with $g(n)$ given by eq 2. Figure 2 shows the results for $\lambda = 1$. The inverse scattering function is plotted for four values of χN, including the critical point. As χN increases, the scattering function gets closer to divergence until the critical point is reached at $(\chi N)_c = 29.25$, where $S^{-1}(x_c) = 0$. The critical lamellar spacing L_c was derived from the critical wavevector k_c by using the following expression:

$$x_c = k_c^2 R_g^2 = \left(\frac{2\pi}{L_c}\right)^2 R_g^2 \tag{17}$$

For $\lambda = 1$ we find $L_c/R_g = 3.41$. For $\lambda = 0$, the Leibler result was recovered and the critical point is at $(\chi N)_c = 10.495$ and $L_c/R_g = 3.23$. The critical point for the linear gradient copolymer with $\lambda = 0.5$ was found in a similar manner by adding in the effects of the pure A and pure B ends.[6] The critical point is at $(\chi N)_c = 13.86$ and $L_c/R_g = 3.33$.

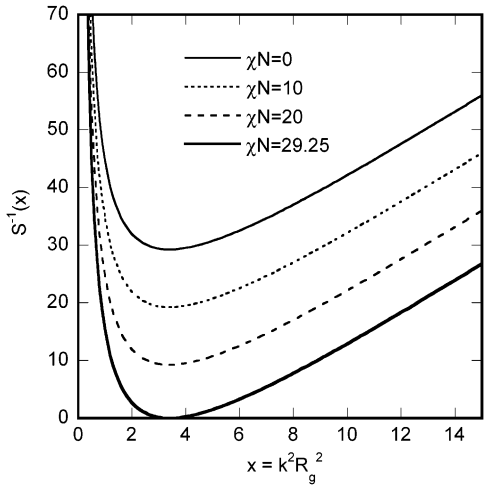

Figure 2. Inverse scattering functions for $\lambda = 1$. The magnitude of the scattering function increases as χN increases and diverges at the critical point: $(\chi N)_c = 29.25$.

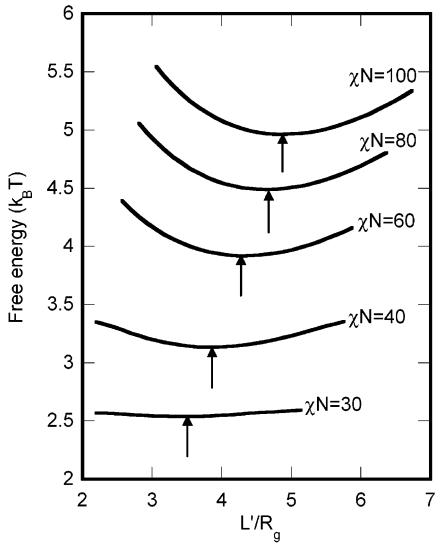

Figure 3. Free energy per chain as a function of repeat length. The minimum represents the equilibrium repeat distance for the specified value of χN.

The hyperbolic tangent profile requires numerical integration and was used previously in the work of Aksimentiev and Holyst.[26] Aksimentiev has provided the critical point calculation for a tanh gradient copolymer with $\lambda = 0.5$ and found it to be at $(\chi N)_c = 17.92$ and $L_c/R_g = 3.35$.[27] All four of the critical points have been added to the plot of L/R_g as a function of χN as discussed in the following section. These spinodal transition points fall, as expected, just below the lowest points in the ordered regime that have a detectable minimum in the free energy.

Ordered Region. The dependence of the equilibrium repeat period on λ and χN was determined in the ordered lamellar region. To find the equilibrium repeat distance, the free energy curves were plotted as in Figure 3. At a given χN and a range of system sizes L', the SCMF method was used to find the free energy per chain. When the free energy is plotted as a function of the length of the system in the z direction, a minimum is seen. Since each calculation spans one lamellar repeat, the minimum is the equilibrium repeat length L of the lamellae. This is repeated for a series of values of χN for each of the four copolymers. The free energy

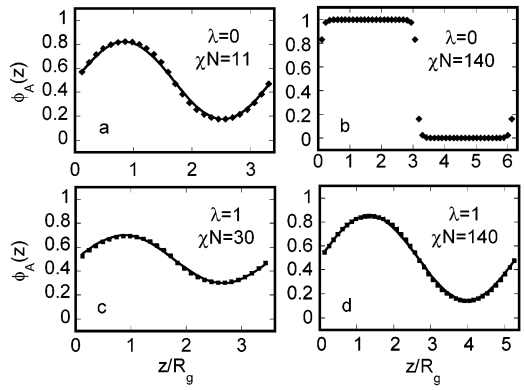

Figure 4. Equilibrium lamellar composition profiles in the weak and strong segregation regimes for block and gradient copolymers: (a) $\lambda = 0$, $\chi N = 11$, $L/R_g = 3.31$; (b) $\lambda = 0$, $\chi N = 140$, $L/R_g = 6.12$; (c) $\lambda = 1$, $\chi N = 30$, $L/R_g = 3.43$; and (d) $\lambda = 1$, $\chi N = 140$, $L/R_g = 5.27$. The solid lines are sinusoidal fits of the data.

curves in Figure 3 are for a linear gradient copolymer with $\lambda = 1$. The lengths are all normalized by R_g with $N = 400$, a value that is large enough to remove the dependence on the specific value of N that was chosen.

At each χN in the ordered lamellar region for which we find the equilibrium repeat length, the SCMF calculations also produce volume fraction profiles. Each calculation results in a lamellar repeat of one A layer and one B layer, and the profiles in Figure 4 are all shown at the equilibrium length of those two layers for that χN. The density variations are sinusoidal, so the profiles are shown with sinusoidal fits of the form:

$$\phi_A(z) = 0.5 + 0.5A \sin\left(\frac{2\pi z}{L}\right) \qquad (18)$$

The amplitude A of the sine wave varies from $A = 0$ for no fluctuations to $A = 1$ for fully saturated A and B layers.

The block copolymer profile at $\chi N = 11$, just above the critical transition, is sinusoidal in form with a modest amplitude, but as χN increases, the segregation between A and B repeat units becomes strong very quickly. At $\chi N = 20$, the profile is no longer sinusoidal, and for $\chi N > 30$ segregation into nearly pure A and B layers is observed. For all of the copolymers, the profiles are sinusoidal with small amplitudes in the weak segregation region at χN close to $(\chi N)_c$. However, the gradient copolymer profiles show "weaker segregation" even at high χN. For $\lambda = 0.5$ with a linear gradient, the profile starts to deviate from a sinusoidal shape at $\chi N = 70$. For $\lambda = 1$, the profile remains sinusoidal even at very high χN, shown here at $\chi N = 140$. This is demonstrated in Figure 4. Just above the order−disorder transition, $\chi N = 11$ for $\lambda = 0$ in Figure 4a and $\chi N = 30$ for $\lambda = 1$ in Figure 4c; the profiles are both sinusoidal. In the strong segregation regime, at $\chi N = 140$ in Figure 4b and 4d, the profiles for the two melts are very different. In this region, the gradient copolymer amplitude remains small and the profile is sinusoidal in form. The block copolymer amplitude is saturated at $A = 1$, and the interfacial region is very narrow, with a width equivalent to only two or three statistical segment lengths. These results are summarized in Figure 5, where the amplitude of the composition modulation is shown as a function of χN for all four copolymers. The χN data for each copolymer are normalized to the critical point and are shown on a log scale. In each case, the

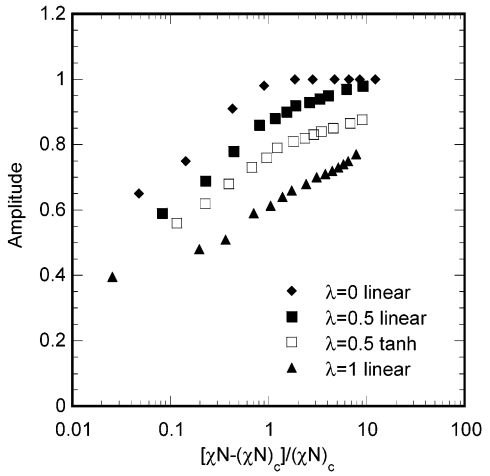

Figure 5. Amplitude of the sine wave fit in eq 18 to the composition profile for four copolymers as a function of normalized χN.

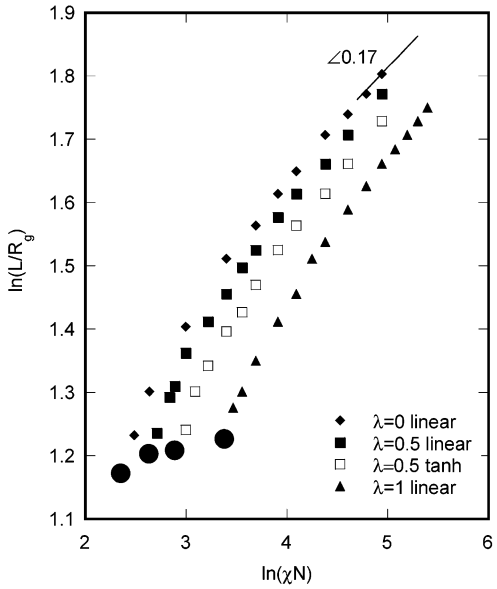

Figure 6. Equilibrium repeat distance as a function of χN for four copolymers. The solid circles are the calculated critical order−disorder transition points for each copolymer.

amplitude approaches $A = 1$ logarithmically and then levels off when the polymers become strongly segregated as in Figure 4b.

The equilibrium repeat distances for each copolymer are plotted as a function of χN in Figure 6. From this plot, scaling relationships of the following form are seen for high values of χN:

$$\frac{L}{R_g} \propto (\chi N)^{\nu} \tag{19}$$

For the block copolymer ($\lambda = 0$) this plot demonstrates the familiar scaling law for the strong segregation regime as determined by the narrow interphase approximation, $\nu = {}^1/_6$.[12] The data also match an approximation for the weak segregation regime as determined by an order parameter expansion by Mayes and Olvera de la Cruz that gives ν in the range 0.45−0.5.[28−30] The gradient copolymers exhibit similar behavior, but in the region shown the scaling exponents are slightly higher in the strong segregation regime. For the gradient copolymer with $\lambda = 1$, the exponent is close

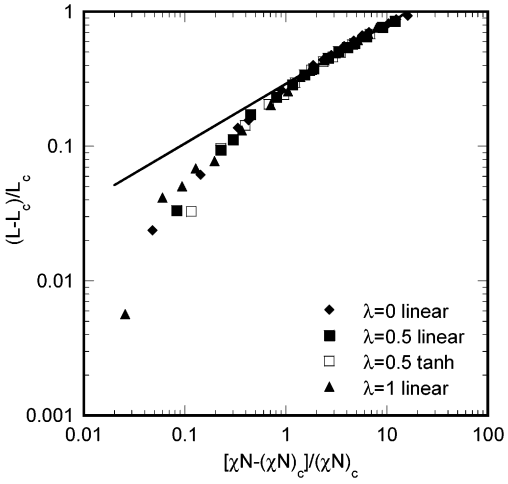

Figure 7. Normalized L vs normalized χN for a series of copolymers with different values of gradients λ. The line is the power law fit to the data given in eq 20.

to 0.2 but is still decreasing slowly. As expected, with increasing composition gradient in the chain, a greater repulsive χN is required to achieve a given separation. A very high χN would be required to achieve the same repeat period for $\lambda = 1$ that is seen in block copolymers. This result is in accordance with the observation that the volume fraction profiles show weaker segregation at high χN in gradient copolymers.

Because the four copolymers exhibit similar qualitative behavior after their respective transitions to the ordered region, it is also interesting to look at these data renormalized to the critical points. Figure 7 shows L normalized to L_c as a function of χN normalized to $(\chi N)_c$. The points all fall on a universal curve, and the scaling behavior is the same for all four copolymers regardless of λ or the type of gradient. For larger χN, the data follow a power law relationship given by

$$\frac{L - L_c}{L_c} = 0.2919\left[\frac{\chi N - (\chi N)_c}{(\chi N)_c}\right]^{0.4427} \tag{20}$$

The power law fit is based on the whole range of data for $\lambda = 0$ and fits well in the strong segregation region but overestimates in the region just above the critical transition.

The influence of fluctuations on the universality of the gradient copolymer mean-field results is an interesting question. Fluctuations are known to modify the transition near the mean-field critical point in copolymers of finite size N. The leading order corrections to the mean-field critical value of χN in block copolymer melts scale as $1/N^{1/3}$. Though the coefficient will change for gradient copolymers, the scaling with N is expected to be similar. Fluctuation effects can be analyzed using more robust field theoretical methods[31] and/or simulations and could be a subject of possible future study.

Conclusions

Gradient copolymers undergo microphase separation like block copolymers and form lamellar structures in the symmetric case. The transition from the disordered to the ordered phase with increasing χN is brought on by increasing correlations in composition fluctuations that eventually overcome entropic forces to form a periodic structure. The disordered state is characterized by the scattering function, which can be accessed

analytically using the random phase approximation to pinpoint the location of the order−disorder transition. In the ordered lamellar state, self-consistent mean-field calculations allow the periodic structure to be characterized by finding equilibrium repeat distances and composition profiles across the interfaces. The SCMF and RPA techniques were used to look at the phase segregation behavior of four symmetric A−B copolymers: a block copolymer, two linear gradient copolymers, and a tanh gradient copolymer.

The critical point was found for all four copolymers by locating the divergence in the RPA scattering function. The equilibrium lamellar repeat distance for the ordered phase was found using SCMF calculations. For a fixed value of χN, increasing the width of the composition gradient along the chain decreases the lamellar repeat length. In both cases, it is clear that a gradient in composition along the chain makes phase separation more difficult than for a block copolymer. For example, in block copolymer melts, the order−disorder transition is known to occur at $(\chi N)_c = 10.495$. For a fully tapered gradient copolymer melt with $\lambda = 1$, phase separation is more difficult, and the critical point is raised to $(\chi N)_c = 29.25$.

The composition profile across the A and B layers was calculated using SCMF theory. For all four copolymers, the profiles are sinusoidal in form at values of χN just above the critical transition. For block copolymers the profiles quickly deviate from a sine waveform with increasing χN. However, the gradient copolymers with $\lambda = 1$ have profiles that remain sinusoidal even at very high χN. Gradient copolymers offer a large degree of control over the A−B interfacial profile, and thus they may be very useful in applications where interfacial properties are important. For example, the vibration damping properties of a polymeric material in the high-frequency range are coupled to the glass transition, which is expected to be very broad for a gradient copolymer with $\lambda \approx 1$ in the case where the A and B homopolymers have very different glass transition temperatures.

The dependence of the equilibrium repeat length (normalized by R_g) on χN is often studied as a power law. It is widely accepted that block copolymers in the strong segregation limit have a power law exponent of $\nu = {}^1/_6$. Gradient copolymers seem to exhibit slightly different behavior, but upon renormalization to their respective critical points, we found that the scaling behavior is universal across a wide range in χN, regardless of λ or the type of gradient.

Acknowledgment. This work was supported by the MRSEC program of the National Science Foundation (DMR-0076097) at the Materials Research Center of Northwestern University. Partial support for M.D.L. from the Clare Boothe Luce Graduate Research Fellowship is also acknowledged. We gratefully thank Aleksei Aksimentiev for doing the numerical calculation of the hyperbolic tangent gradient copolymer critical point.

References and Notes

(1) Bates, F. S.; Fredrickson, G. H. *Annu. Rev. Phys. Chem.* **1990**, *41*, 525.
(2) Fasolka, M. J.; Mayes, A. M. *Annu. Rev. Mater. Res.* **2001**, *31*, 323.
(3) Matsen, M. W. *J. Phys.: Condens. Matter* **2002**, *14*, R21.
(4) Shakhnovich, E. I.; Gutin, A. M. *J. Phys. (Paris)* **1989**, *50*, 1843.
(5) Fredrickson, G. H.; Milner, S. T.; Leibler, L. *Macromolecules* **1992**, *25*, 6341.
(6) Mayes, A. M.; Olvera de la Cruz, M. *J. Chem. Phys.* **1989**, *91*, 7228.
(7) Dobrynin, A. V.; Erukhimovich, I. Y. *Macromolecules* **1993**, *26*, 276.
(8) Olvera de la Cruz, M.; Sanchez, I. C. *Macromolecules* **1986**, *19*, 2501.
(9) Shinozaki, A.; Jasnow, D.; Balazs, A. C. *Macromolecules* **1994**, *27*, 2496.
(10) Matsen, M. W.; Schick, M. *Macromolecules* **1994**, *27*, 4014.
(11) Leibler, L. *Macromolecules* **1980**, *13*, 1602.
(12) Helfand, E.; Wasserman, Z. R. *Macromolecules* **1976**, *9*, 879.
(13) Wang, J. S.; Matyjaszewski, K. *Macromolecules* **1995**, *28*, 7901.
(14) Patten, T. E.; Matyjaszewski, K. *Adv. Mater.* **1998**, *10*, 901.
(15) Matyjaszewski, K.; Xia, J. H. *Chem. Rev.* **2001**, *101*, 2921.
(16) Hawker, C. J.; Barclay, G. G.; Orellana, A.; Dao, J.; Devonport, W. *Macromolecules* **1996**, *29*, 5245.
(17) Malmstrom, E. E.; Hawker, C. J. *Macromol. Chem. Phys.* **1998**, *199*, 923.
(18) Gray, M. K.; Nguyen, S. T.; Zhou, H.; Torkelson, J. M. *Polym. Prepr.* **2002**, *43*, 112.
(19) Olvera de la Cruz, M. *Phys. Rev. Lett.* **1991**, *67*, 85.
(20) Almdal, K.; Rosedale, J. H.; Bates, F. S.; Wignall, G. D.; Fredrickson, G. H. *Phys. Rev. Lett.* **1990**, *65*, 1112.
(21) Barrat, J. L.; Fredrickson, G. H. *J. Chem. Phys.* **1991**, *95*, 1281.
(22) Edwards, S. F. *Proc. Phys. Soc. London* **1965**, *85*, 613.
(23) Helfand, E. *Macromolecules* **1975**, *8*, 552.
(24) Hong, K. M.; Noolandi, J. *Macromolecules* **1981**, *14*, 727.
(25) Shull, K. R. *Macromolecules* **2002**, *35*, 8631.
(26) Aksimentiev, A.; Holyst, R. *J. Chem. Phys.* **1999**, *111*, 2329.
(27) Aksimentiev, A. Personal communication.
(28) Mayes, A. M.; Olvera de la Cruz, M. *Macromolecules* **1991**, *24*, 3975.
(29) Tang, H.; Freed, K. F. *J. Chem. Phys.* **1991**, *94*, 7554.
(30) Melenkevitz, J.; Muthukumar, M. *Macromolecules* **1991**, *24*, 4199.
(31) Ganesan, V.; Fredrickson, G. H. *Europhys. Lett.* **2001**, *55*, 814.

MA035141A